

New wide-area algorithms for detecting angle instability using synchrophasors

Dongchen Hu and Vaithianathan “Mani” Venkatasubramanian
School of Electrical Engineering and Computer Science
Washington State University, Pullman, WA 99164-2752
Email: mani@eecs.wsu.edu

Abstract

Electric power system is undergoing major technological advances with many new installations of synchrophasors across the North American grid as well in power systems all over the world. Wide-area monitoring system (WAMS) in the Pacific Northwest and the Eastern Interconnection Phasor Project (EIPP) in the eastern grid are examples of such installations. Synchrophasors together with modern communication technology facilitate the monitoring of the current state of the power system including the phase angles of the bus voltages at critical buses in a time-synchronized fashion.

Power system operation is constantly facing contingencies such as from line faults and generator outages. For operational reliability, the system must be able to withstand all credible contingencies, either by itself (for N-1 contingency) or with the help of Special Protection Schemes (SPS) or Remedial Action Schemes (RAS) (for N-2 or worse contingencies). However, when the system is operating under unforeseen conditions or under unusually high stress, the system can experience the angle instability. In that case, the system breaks up into many islands, resulting in large loss of loads and generations and a potential blackout scenario. In this paper, new algorithms are proposed for detecting the emergence of angle instability phenomenon while it is still evolving so that suitable countermeasures can be initiated to prevent the islanding.

The proposed algorithms and the controller detect the fast separation of phase angles among the critical areas automatically by using the synchrophasors, and proceed to mitigate the instability by suitable switching action. Briefly, the algorithms initiate tripping of critical generators in the accelerating part of the system when necessary, and also initiate load shedding in the decelerating part of the system whenever necessary. The novelty of the algorithms is in the fact that all the decisions are made in real-time purely based on the wide-area synchrophasor measurements without any knowledge of the details of the relay actions that may have resulted in the angle stability phenomenon. The concept of a real-time transient energy function method for the large power system is also explored to solve the problem. The paper will discuss the new algorithms along with illustrative examples on standard IEEE test systems.

1. INTRODUCTION

Power systems are large interconnected nonlinear systems where system wide instabilities or collapses can occur when the system is subjected to unusually high stress. Such system-wide blackouts lead to considerable economic costs as well as adverse societal impacts [2]. Therefore, the operational reliability of the electric power system is of fundamental importance to power system operation and planning. Operator actions together with automatic control actions are designed to prevent or minimize the damage caused by such outages.

Over the past few decades, the power-flows across distant parts of the system have been growing steadily to meet the ever-increasing consumer demands. However, the construction of new transmission lines has been lagging behind because of economic as well as environmental concerns. It is well known that heavy power-flows across long transmission lines weakens the operational security of the power system with respect to oscillatory and angle instability phenomena. In essence, the steady growth of consumer demands with little new transmission support is gradually pushing the electric power system operation closer and closer towards the instability limits. As a consequence, the system operation can find itself close to or outside the secure operating limits under severe contingencies [2-3].

From the technology perspective, there has been a spectacular growth in the past twenty years from advances in computer and communication sciences. Together with the emergence of the synchrophasor technology, these advances provide the opportunity for feasible and economical implementation of wide-area controls in the large electric power system. Many recent publications have analyzed the requirements and designs of wide-area controls. The setup and applications of comprehensive wide-area systems are introduced in [6-9].

One of the earliest applications of wide-area feedback control in the power system is the load frequency control [4] that was developed in the 1970's. Any imbalance between generation and load will cause the deviation of the system frequency away from the nominal 60 Hz. A secondary control loop, called the Automatic Generation Control, (AGC), coordinates the individual governor responses of the generators to regulate the system frequency and also maintain the power exchanges between several control areas. The control center gathers the relevant frequency and power-flow information from across the control area and sends the appropriate set-point adjustments for each of the governor units in the AGC control loop. This AGC control is a slow control system where the wide-area control adjustments are changed every 15 to 30 seconds or so.

The wide-area controls for the voltage control called Secondary Voltage Control schemes are proposed in [6], [10-15]. These papers present the control schemes designed to manage the voltage and reactive power issues all around a wide transmission network. The main objective of the secondary voltage control is to adjust and to maintain the voltage profile inside a network area. Another objective is the control of reactive

generation and flows. This type of control includes the modification of the set-point values of Automatic Voltage Regulation (AVR), the switching of compensation devices, and the change of tap position on transformers. The voltages of key buses are monitored and the control voltage set-points are sent to the local voltage controllers. New approaches for automatic voltage control was proposed in [15] that was motivated toward implementation in the transmission network operated by the Bonneville Power Administration (BPA) in the Pacific Northwest. Again, the secondary voltage control is also a slow control system with time constants ranging from 30 seconds to several minutes.

Advanced protection schemes, called Special Protection Schemes (SPS's) or Remedial Action Schemes (RAS's), have also been developed in recent years. These schemes are designed to detect abnormal system conditions such as simultaneous loss of multiple transmission lines from appropriate relay actions, and to take predetermined corrective actions to prevent the system-wide instability. RAS schemes involve actions such as generation tripping, load shedding, capacitor insertion or dynamic brake insertion, which are enforced at remote substations away from the fault location or other events. The use of SPS/RAS can increase the security of power systems, especially for specific multiple line openings if they are designed properly and if they operate correctly. But these schemes are not flexible, since they require dedicated communication links and extensive off-line tuning calculations. In [16], a method for an adaptive RAS was proposed. The method calculates the difference of potential energy to determine each RAS action to increase the stability of the system, based on the transient energy analysis.

Most of current algorithms used in the wide-area control are based on measurements of bus voltages and generator reactive power [9]. In some applications, it will be more effective to use the phase angle measurements to detect the angle instability, especially, the first swing instability in power systems [4]. Fast exchange of Phasor Measurement Units (PMU) among West Electricity Coordination Control (WECC) utilities is being pursued, and it is reasonable to assume the availability of system wide phase angle information (from specific PMU locations) in the near future [9]. This paper proposes new algorithms that detect and mitigate transient instability by utilizing the phase angle measurements and frequency measurements of critical generator bus high side voltages from across the entire power system.

All the simulations mentioned in this paper are done using the Transient Security Assessment Tool (TSAT). TSAT is a software tool jointly developed by Powertech Labs Inc. and Nanjing Automation Research Institute.

The paper is organized as follows. The algorithm using the system wide phase angles is described in Section 2, and the simulation results are also illustrated in this section. In Section 3, the second algorithm using the concept of real-time energy function is introduced together with the simulation results. A more detailed discussion of the results in this paper can be seen in the recent Masters thesis [1].

2. ALGORITHM BASED ON THE PHASE ANGLES

2.1. INTRODUCTION

A first version of the phase angle based algorithm was postulated in Appendix 3 of the recent paper [9]. This section will discuss the new algorithm in more detail along with illustrative examples on standard IEEE test systems. These algorithms thus extend the framework of Wide-Area Control Systems (WACS) controller [9] previously developed at Bonneville Power Administration and Washington State University by including phase angles into the algorithm computations.

2.2. ALGORITHM

The proposed algorithm extends the concept of the voltage-based algorithm Vmag from [9] by consideration of the phase angle measurements. Briefly, the algorithm Vmag in [9] measured the severity of disturbances in the WECC system by quantifying the area of the voltage dips below pre-specified thresholds during system swings. The phase angle algorithm of this section analyzes the phase angles of the system in a similar fashion. The consideration of the phase angles is more challenging as compared to voltage magnitudes because the phase angles can vary over wide ranges during the system operation. While the voltage magnitudes are kept within tight tolerances under normal system conditions, the phase angles and the relative phase differences can vary a lot across the system as determined by the MW power transfers and the availability of transmission paths for the power transfer. In order to handle this difficulty, we propose the concept of a real-time center of inertia for the computation of the system phase angle reference [9] that is used to quantify the extent of phase angle variations away from the system center.

At present, the algorithm analyzes the phase angles in two stages: 1) the angle stability within each control area, and, 2) the angle stability of the entire large system. The principle in each step is similar.

First, let us recall the definition of the Center of Angles (COA) [4],

$$\delta_{COA} = \frac{\sum_{i=1}^N \bar{\delta}_i H_i}{\sum_{i=1}^N H_i} \quad (2.1)$$

where $\bar{\delta}_i$ is the internal machine rotor angle and H_i is the respective generator inertia time constant. Since the internal machine rotor angle cannot be directly measured, we approximate the internal angle with the phase angle of the high side bus voltage, which is normally monitored by synchrophasors. Similarly, the inertia time constant H_i in (2.1) is difficult to access in real-time. Therefore, we substitute the weights defined by the inertia constants in (2.1) with the high side active power injections for the generators.

The machine inertias are typically proportional to the real power outputs. The modified formula (2.2) presented below is thus readily suited for real-time computation using the synchrophasors.

Let us assume the availability of the phase angle measurements, say, δ_j^i , from a few key generating plants, say for $j=1,2,\dots,N$ in an area i . Then, we introduce the notion of the approximate center of inertia angle reference for the area, say, δ_c^i , by the rule,

$$\delta_c^i = \frac{\sum_{j=1}^N \delta_j^i P_j^i}{\sum_{j=1}^N P_j^i} \quad (2.2)$$

where P_j^i denotes the current MW generation schedule at the plant j in area i . By increasing the number of angle measurements within each area, we can improve the accuracy of the computation of the angle reference δ_c^i and we can also improve the redundancy. Also, this rule (2.2) is inherently tolerant of loss of one or more PMU channels as is commonly the case in the real-time framework. Similarly, the center of inertia angle reference for the entire system, denoted δ_c , can be computed with the rule,

$$\delta_c = \frac{\sum_{i=1}^N \delta_c^i P^i}{\sum_{i=1}^N P^i} \quad (2.3)$$

where N is the total number of areas that are available in the control formulation, and P^i denotes the current total generation in Area i . The latest total load P^i of area i is readily available from the routine AGC calculations.

Next, we present a heuristic rule for detecting angle instability using these concepts in a real-time framework. When the representative angle δ_c^i of an area in (2.2) continuously increases away from the center of inertia δ_c beyond a pre-specified metric, we would heuristically interpret that Area i is moving towards separation from the rest of the system. In this case, a suitable remedial action could be the tripping of generation in that area. Similarly, when the angle δ_c^i continues to decrease beyond a predefined threshold, we would interpret that as a likely separation of Area i that could be countered by load shedding in Area i . These rules need to be crosschecked by analyzing the respective frequency measurements.

In our studies, we set the control trigger heuristics to be similar to the voltage error algorithm Vmag [9]. In the case of phase angles, we define $\Delta\delta_c^i = \delta_c^i - \delta_c$. We then accumulate two integral terms, denoted Ω_a^i and Ω_u^i , respectively, to denote the speeding

up or slowing down of Area i with respect to the center of inertia reference frame. First, the term Ω_a^i is the integral for $\Delta\delta_c^i$, whenever $\Delta\delta_c^i$ continuously stays above a threshold, say $\Delta\delta_c^{i*}$. The accumulated error Ω_a^i is reset to zero whenever the angle $\Delta\delta_c^i$ drifts below $\Delta\delta_c^{i*}$. When Ω_a^i grows above a pre-specified value, say Ω_a^{i*} , the Area i is interpreted to be speeding away from the rest of the system and a suitable generation tripping may be initiated in that area. The value of Ω_a^{i*} will be tuned in real-time based on the current total generation and the current spinning reserve in Area i . That is, the smaller the current spinning reserve (relative to the total generation) in Area i , then the lower the threshold value for Ω_a^{i*} . The computation of the Ω_d^i is then similar to accumulating the integral of $\Delta\delta_c^i$ below a threshold, denoted $\Delta\delta_d^{i*}$. When Ω_d^i grows above a pre-specified value, say Ω_d^{i*} , load shedding in Area i may be initiated to mitigate the disturbance event.

2.3. ILLUSTRATION OF THE ALGORITHM USING THE TWO AREA SYSTEM

We implement the above algorithm in the Kundur two area system [4] (the diagram of the two area system is shown in Appendix A). The system is simply divided into two areas with Gen 1 and Gen 2 in Area 1, Gen 3 and Gen 4 in Area 2, respectively. We define

$$\delta_c^1 = \frac{\delta_1^1 P_{G1} + \delta_1^2 P_{G2}}{P_{G1} + P_{G2}} \quad (2.4)$$

$$\delta_c^2 = \frac{\delta_2^3 P_{G3} + \delta_2^4 P_{G4}}{P_{G3} + P_{G4}} \quad (2.5)$$

where δ_1^1 , δ_1^2 , δ_2^3 , δ_2^4 are the phase angles of the bus voltage of the four generators, respectively. Also, we define

$$\delta_c = \frac{\delta_1^1 P_{G1} + \delta_1^2 P_{G2} + \delta_2^3 P_{G3} + \delta_2^4 P_{G4}}{P_{G1} + P_{G2} + P_{G3} + P_{G4}} \quad (2.6)$$

$$\Delta\delta_c^1 = \delta_c^1 - \delta_c, \quad \Delta\delta_c^2 = \delta_c^2 - \delta_c \quad (2.7)$$

When we apply a three phase fault at BUS 8 and after some certain time we clear the fault and remove three of the four lines between BUS 7 and BUS 8 at time 0.1 sec, the details of the simulation results are shown below. When the fault-on time is set to be 0.08 sec, 0.10 sec, and 0.11 sec, the curves of $\Delta\delta_c^1$ and $\Delta\delta_c^2$ are shown in Figure 2-1, Figure 2-2 and Figure 2-3, respectively. Figure 2-4 shows the curve of $\Delta\delta_c^1$ near 60 degrees for the simulation in Figure 2.3.

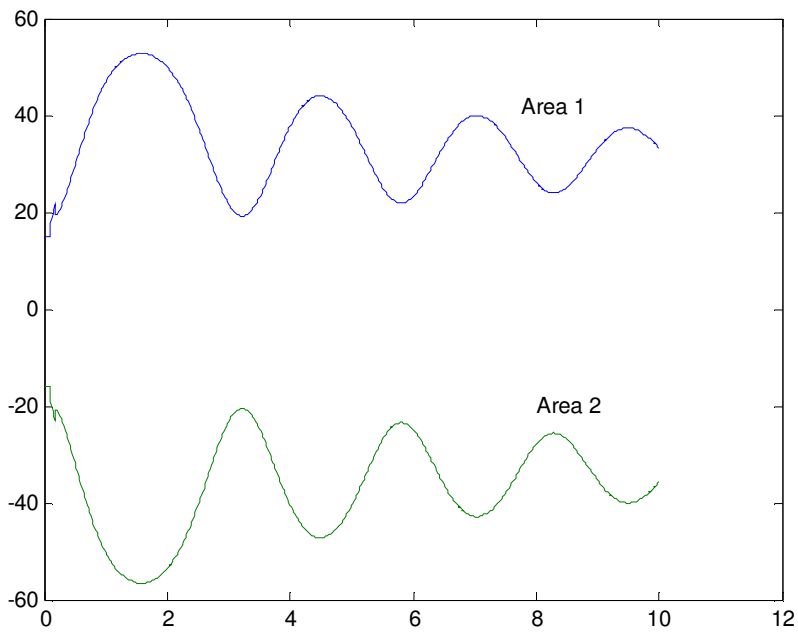


Figure 2-1 Angles of each area (fault-on time=0.08 sec)

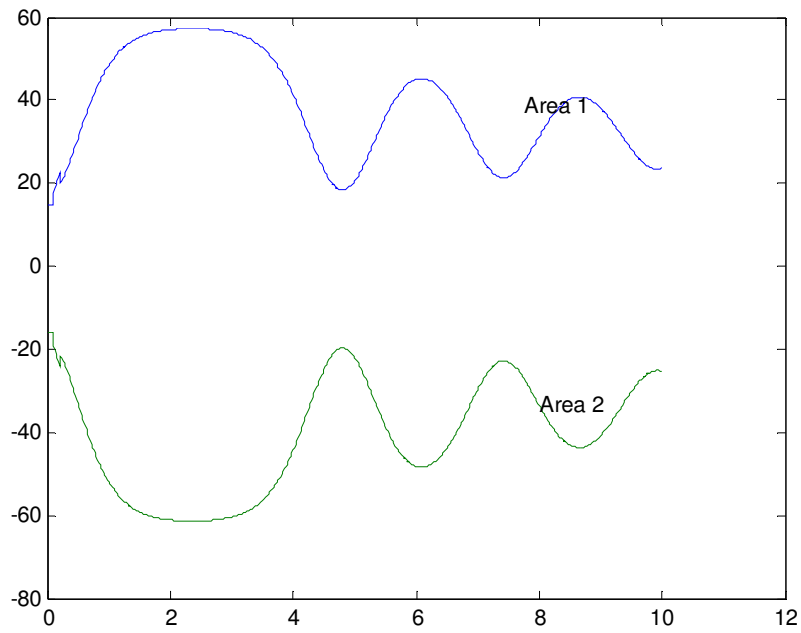


Figure 2-2 Angles of each area (fault-on time=0.10 sec)

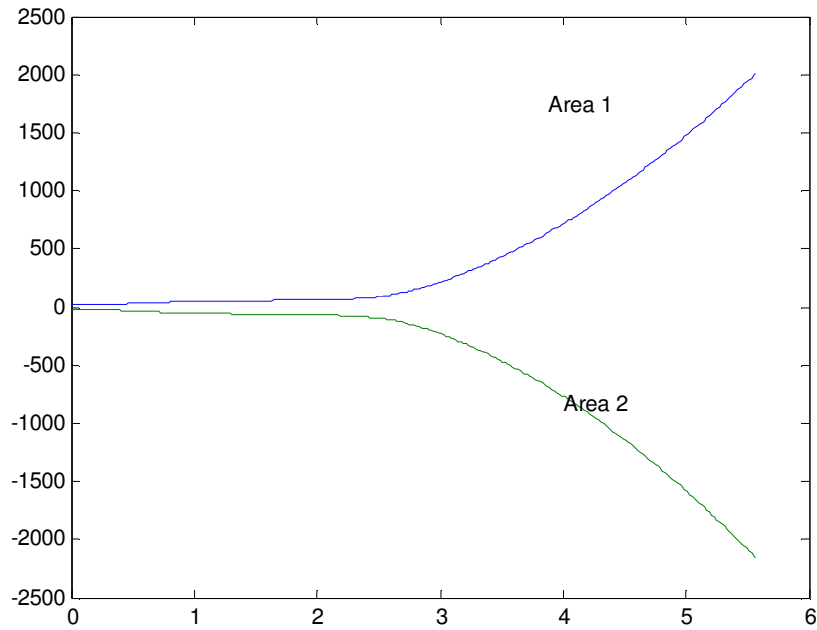


Figure 2-3 Angles of each area (fault-on time=0.11 sec)

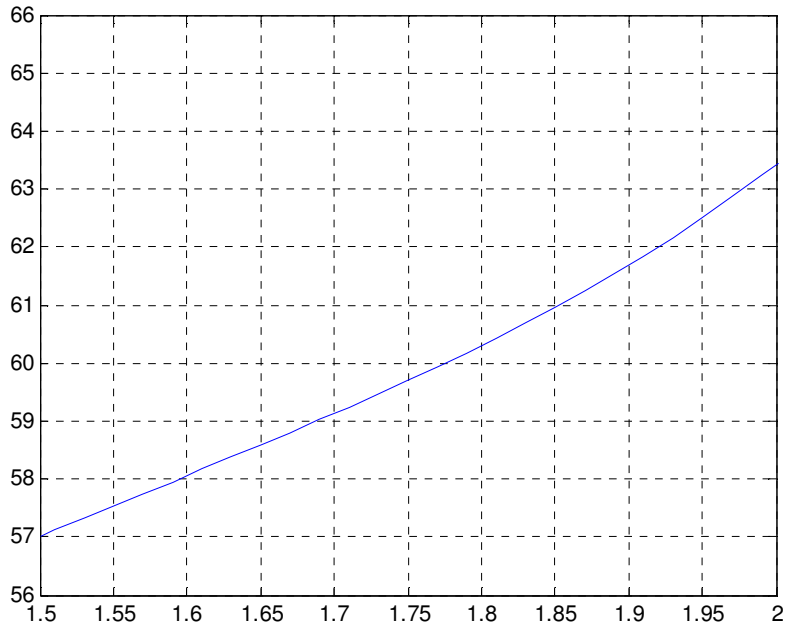


Figure 2-4 Angles of area 1 (fault-on time=0.11 sec)

From the cases above, we could say that 0.10 sec is the critical fault time for this three-phase fault on Bus 8. Looking into Figure 2-2, we could find that the maximum value of $\Delta\delta_c^1$ is 57.3 degrees and the minimum value of $\Delta\delta_c^2$ is -61.5 degrees for the critically stable case. Therefore, we set the conservative values, $\Delta\delta_a^* = 60$ degrees,

and $\Delta\delta_d^* = -65$ degrees. Similarly, we can estimate the values $\Omega_a^* = 5$ and $\Omega_d^* = -5$ from additional studies. Simulation results with different fault-on times are shown in Table 2-1. From the results, we could say Area 1 is moving away from the system earlier than Area 2. When we try to trip some generation of Area 1, we find that the generation tripping action by itself is not enough to stabilize the system. Therefore, we initiate some load shedding action in Area 2 which is decelerating from the center of the system. We trip Gen 1 and 50% of the load at Bus 9 at time 1.83 sec for the second case in Table 2-1. After the control actions, the system can be stabilized as shown in Figure 2-5. Also, if we trip Gen 1 at time 1.83 sec and 50% load at Bus 9 at time 1.93 sec, the system can still be stabilized.

Table 2-2 summarizes the benefits provided by the algorithm in improving the transient stability. Taking the first case as example, the critical clearing time without the proposed control is 0.10 seconds (the first entry in Table 2-1). The system becomes transient stable for the clearing time of 0.11 seconds as well as 0.12 seconds. With the automatic generation and load tripping control as proposed, the critical clearing time improves to 0.14 seconds. Compared to the 0.10 seconds for the original system with no control, the automatic controller as proposed provides an improved critical clearing time by a margin of 0.04 seconds (2.4 cycles). These simulations illustrate the fact that the controller as proposed is useful for the two-area system in improving the transient stability of the system for critical contingencies.

Table 2-1 Simulation results for the two-area system

Fault Time	0.10 sec	0.11 sec		0.12 sec	
Stability	Stable	Unstable		Unstable	
Area		Area1	Area2	Area1	Area2
T_start		1.73 sec	1.89 sec	1.52 sec	1.61sec
T_control		1.83 sec	1.93 sec	1.62 sec	1.69 sec
Int		6.0525	-5.2325	6.0965	-5.3345
T_unst		2.4 sec		2.0 sec	

T_start is the time $\Delta\delta_a^1$ increases beyond $\Delta\delta_a^{1}$; T_control is the time Ω_a^1 reaches Ω_a^{1*} ; Int is the value of Ω_a^1 at T_control. T_unst is the time $\Delta\delta_c^1$ reaches 90 degrees.

In Table 2-1, the time duration between T_start (the time the phase angle goes above the threshold) and T_control (the time the control trigger is issued) can be used to quantify the severity of the disturbance. If the time duration $T_{control} - T_{start} > T^*$, we can interpret the angle instability to be severe which will be controlled by only generator tripping, whereas if $T_{control} - T_{start} < T^*$, both generation tripping and load shedding will be initiated. For the two-area system, we can use a value of say 7 cycles or 0.117 sec for the value of T^* . Further investigation on the tuning of T^* is recommended.

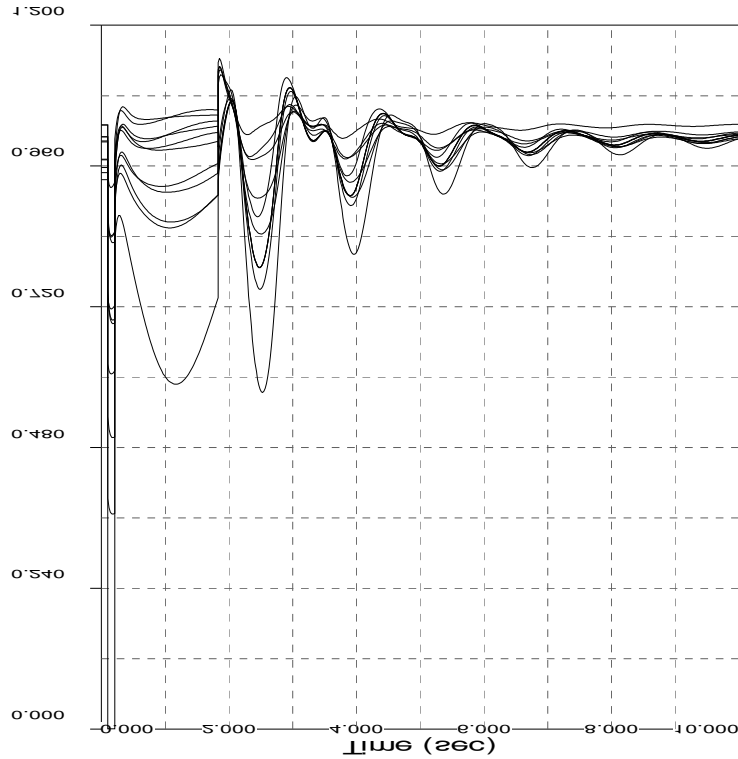


Figure 2-5 Bus voltages with tripping actions at same time (fault-on time=0.11 sec)

Table 2-2 Improvement on the system stability

Fault Bus	Line Removed	Fault Time (cycle) improvement
8	7-8	2.4
7	7-8	1.8

Tests in the two-area system lead to some discussions of the new algorithm.

(1) If we use inertia constants to compute δ_c as formula (2.1) shows, with the 0.11 sec-fault time, Figure 2-6 shows the comparison of the two methods. It shows that the substitution with power output in place of the inertia constant to compute the center of the system angle δ_c is reasonable.

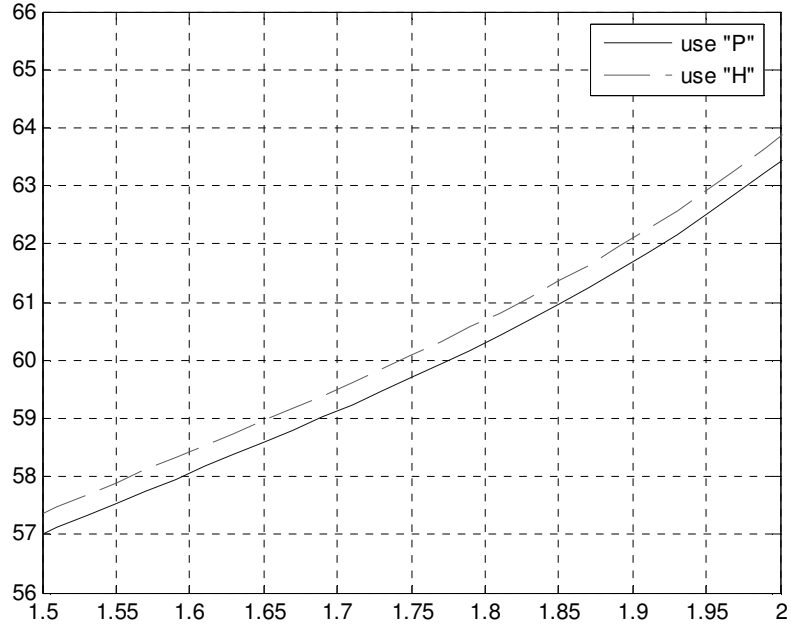


Figure 2-6 comparison of two ways to compute δ_c (fault-on time=0.11 sec)

(2) The thresholds are set up based on the critical cases and they need to be tuned in order to make the algorithm work reasonably for diverse conditions.

(3) Control actions such as the generation tripping in the accelerating area or load shedding in the decelerating area are the normal methods in system protection. But, the tripping or shedding amounts still need to be determined from further studies in future research works.

2.4. IMPLEMENTATION OF THE ALGORITHM IN THE 39 BUS SYSTEM

We also implement the algorithm in the 39 bus New England system (the diagram of the 39 bus system is shown in Appendix B). In this system, we assume that each generator bus represents an individual control area, thus, the algorithm is re-written as follows:

1) The COI of the system is defined as,

$$\delta_c = \frac{\sum_{j=1}^{10} \delta_j P_j}{\sum_{j=1}^{10} P_j}, \quad j \text{ is the number of the generator.} \quad (2.8)$$

2) In case of phase angles, we define $\Delta\delta_j = \delta_j - \delta_c$

3) The term Ω_a^j is the integral for $\Delta\delta_j$, whenever $\Delta\delta_j$ continuously stays above a

threshold, say $\Delta\delta_a^*$. The accumulated error Ω_a^j is reset to zero whenever the angle $\Delta\delta_j$ drifts below $\Delta\delta_a^*$. When Ω_a^j grows above a pre-specified value Ω_a^* , the generator j is interpreted to be speeding away from the rest of the system and a suitable generation tripping may be initiated to that generator. The computation of the value Ω_d^j is then similar to accumulating the integral of $\Delta\delta_j$ below a threshold, denoted $\Delta\delta_d^*$. When Ω_d^j grows above a pre-specified value, say Ω_d^* , load shedding in generator bus j may be initiated to mitigate the disturbance event, or, if the frequency of the generator j is above 60Hz, we need to trip this generator instead of load shedding.

4) In the 39 bus system, the threshold $\Delta\delta_a^*$ is set to be 60 degrees, $\Delta\delta_d^*$ is set to be -70 degrees. These two thresholds are set up based on the observation of the boundary of phase angles in critical cases and the thresholds are also tested for most of routine the faults in the test system. The settings Ω_a^* and Ω_d^* are set to be 5 and -5 respectively.

Now, we introduce an example to illustrate the algorithm. There is a fault near Bus 4 on the line 4-14, and line 4-14 is removed after fault clearing. When the fault time is set to be 12 cycles, Figure 2-7 shows $\Delta\delta_j$ of each generator in the system and the system is classified to be stable. When the fault time is set to be 13 cycles, the figure of phase angles is shown below (Figure 2-8).

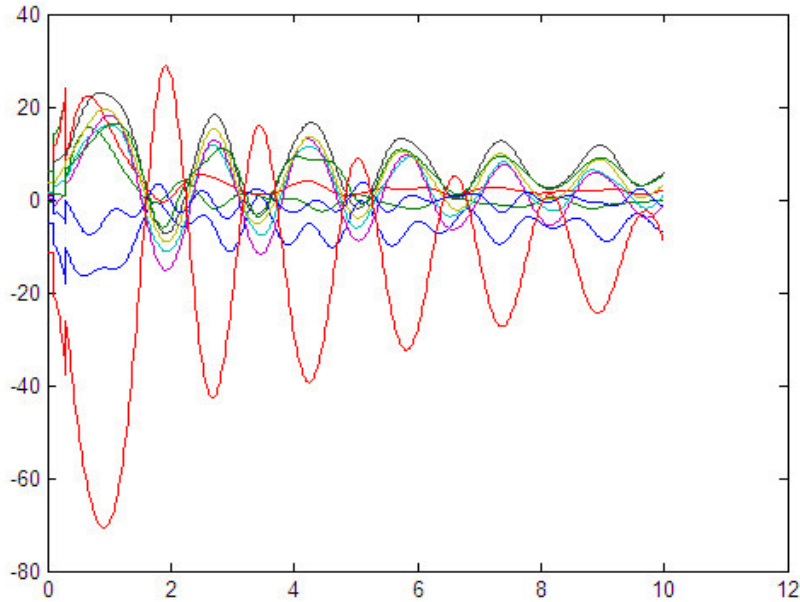


Figure 2-7 Angles of generators (fault-on time=12 cycles)

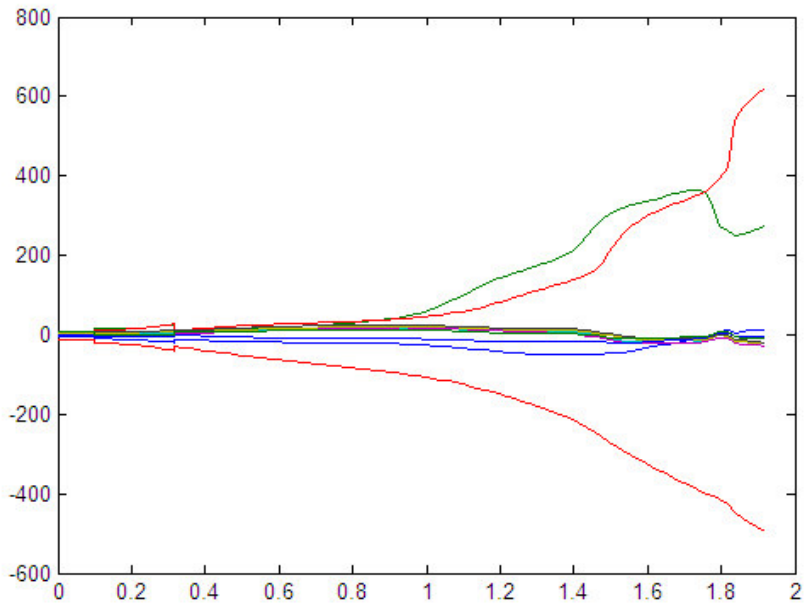


Figure 2-8 Angles of generators (fault-on time=13 cycles)

From the algorithm, generator 10 is the first to move away from the COA, the control time is 0.76 sec. Therefore, we trip Gen 10 to stabilize the system as the frequency of Gen 10 is above 60 Hz (Figure 2-8). The figure of the system bus voltages is shown below (Figure 2-9).

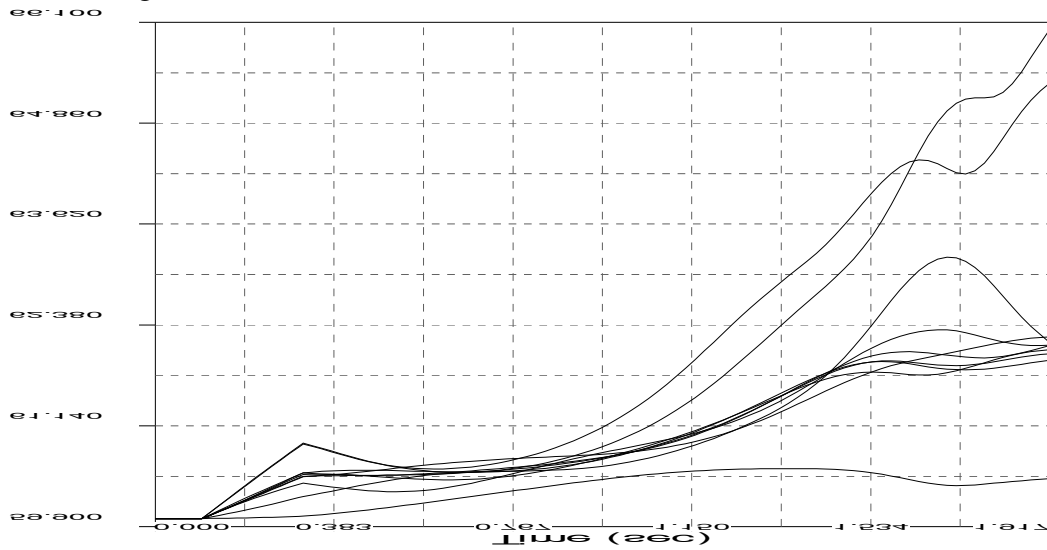


Figure 2-9 Generator speeds (fault-on time=13 cycles)

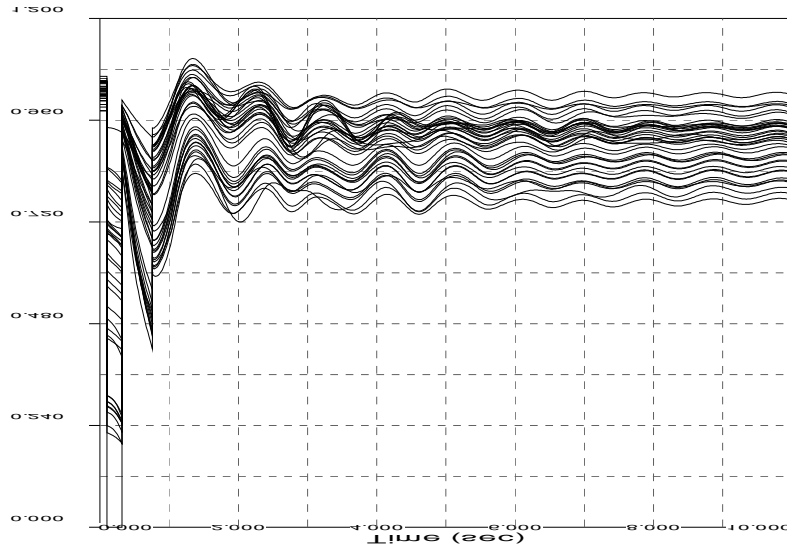


Figure 2-10 Bus voltages after tripping Generator 10 (fault-on time=13 cycles)

The following table (Table 2-3) summarizes the simulation results for various single line outages. The fault time of each fault is the critical time when the system becomes unstable. In the tables, The Gen tripped and the Tripping time denote the generator to be tripped and the tripping time when the algorithm initiates a control action, respectively. And after the generation tripping, the system will become stable.

Table 2-3 Simulation results for the 39 bus system

Fault Bus	Line Removed	Fault Time(cycles)	Gen tripped	Tripping time(sec)
4	4-14	13	10	0.76
14	4-14	13	10	0.78
4	4-5	12	10	0.88
3	3-4	12	10	0.73
4	3-4	11	10	0.84
5	5-6	11	2	0.90
6	5-6	10	2	1.11
2	2-25	7	9	1.06
25	2-25	6	9	0.92
16	16-19	5	4,5	0.52
19	19-16	5	4,5	0.46
21	16-21	9	10	0.90
16	16-21	7	10	0.77

Table 2-4 Improvement on the system stability

Fault Bus	Line Removed	Critical Clearing Time (cycles) improvement
4	4-14	3
14	4-14	3
4	4-5	4
3	3-4	2
4	3-4	4
5	5-6	2
6	5-6	2
2	2-25	3
25	2-25	3
16	16-19	0
19	19-16	0
21	16-21	3
16	16-21	3

Table 2-4 summarizes the benefits provided by the algorithm in improving the transient stability. For instance, let us consider the first contingency in Table 2-4, the three-phase fault near Bus 4 and the loss of line 4-14. The critical clearing time without the proposed control is 12 cycles. For the case of 13 cycles-clearing time, the phase angle based algorithm identifies Gen 10 as the critical generator and a trip signal is issued by the control to Gen 10 at 0.76 seconds (first entry of Table 2-3). Assuming that Gen 10 gets tripped by the proposed controller, the system becomes transient stable for the clearing time of 13 cycles as well as 14 cycles. With the automatic generation tripping control as proposed, the critical clearing time improves to 15 cycles. Compared to the 12 cycles for the original system with no control, the automatic controller as proposed provides an improved critical clearing time by a margin of 3 cycles. Table 2-4 thus illustrates the effectiveness of the algorithm in detecting and mitigating transient stability contingencies in various parts of the system.

It is important to point out that the control decision is entirely based on the measured phase angles and the controller does not know what outage resulted in the observed phase angle responses. This is a purely a response based algorithm in the spirit of the previous algorithms in [9].

From Table 2-4, the controller based only on phase angle improves the system security for all excepting two outages. For the two exceptions, the controller does not cause negative margins or undesirable effects. Thus, the controller does appear to be effective for the 39 bus test system.

2.5. CONCLUSIONS

This section presents the algorithm for processing of phase angle measurements from across the system to decide whether any part or control area within the system is speeding away from the rest. When the angle separations go above preset thresholds, remedial actions such as generation and load tripping are ordered by the stability controller to keep the areas in synchronism. This new algorithm can detect and mitigate transient instability by utilizing the phase angle measurements of critical generator bus voltages. The algorithm has been tested to be effective in the simulation of the two-area system and the 39 bus system. The phase angle thresholds are set up based on the critical cases and tuned in order to make the algorithm work for the whole system. Control actions such as the tripping of generation in accelerating area or shedding of load in decelerating area are the normal methods in system protection. However, if the frequencies of the generators in decelerating area are above 60 Hz, we may need to trip generation in the decelerating area instead of load shedding. The tripping or shedding amounts still need further studies in future research work.

3. ALGORITHM USING THE ENERGY FUNCTION CONCEPT

3.1. BACKGROUND

Transient energy methods are mathematical techniques for analyzing the power system dynamics due to excursions in voltage phase angles and their magnitudes. The energy associated with the deviation from system equilibrium point is quantified as a kinetic energy function (KE) that is related to changes in rotor speeds and a potential energy function (PE) that is connected with changes in relative rotor phase angles. In our research, we are trying to establish the relation between the system transient behavior and the measurements from PMU. The transient energy method is used to analyze the system stability so that PMU based measurements can be used for detecting the system instability in real-time, and for activating suitable control actions.

Figure 3-1 illustrates the equal area stability criterion for “first swing” stability [20]. If the decelerating area (energy) above the mechanical power load line is greater than the accelerating area below the load line, stability can be maintained.

Transient energy analysis has been developed with substantial advances in recent years. The method to evaluate the transient response of a power system following a large disturbance was proposed in [18-24]. [21-22] used energy functions to quantify the energy of a system disturbance. In 1982, Vittal [23] introduced the idea of an individual machine’s energy function, and in 1988 Stanton used transient energy functions of an individual generator, to assess instability of individual sites [24-25]. The Energy Functions are fully described in references such as [21,22,26]. An algorithm using the energy function concept to detect system instability of a transmission tie-line based on PMU can be found in the recent paper [28], where the definition of a critical energy was carried out as criterion of system stability.

In this paper, we apply the energy function concept for a multi-machine power system using the concept of real-time center of angle computation introduced in Section 2. We compute the potential energy as well as the kinetic energy of each machine and define thresholds to decide a) whether the system is progressing towards transient stability and b) to identify the critical generator.

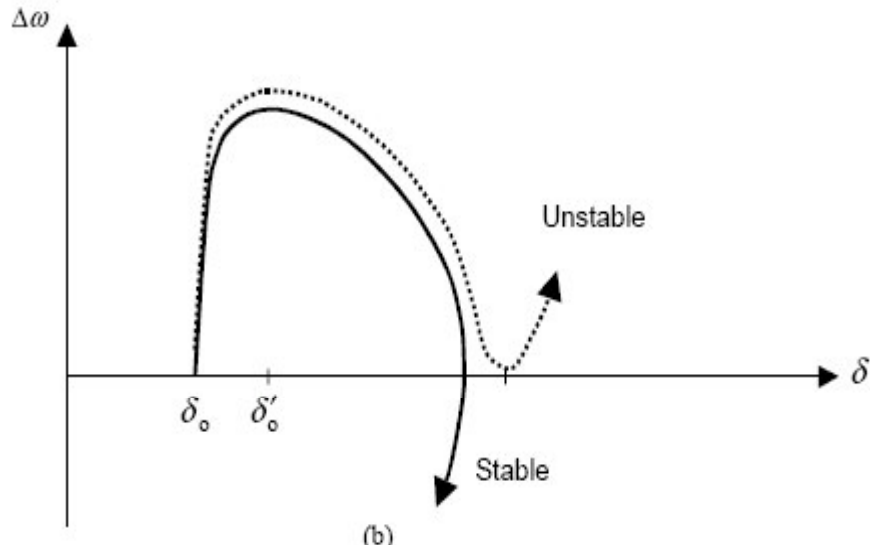
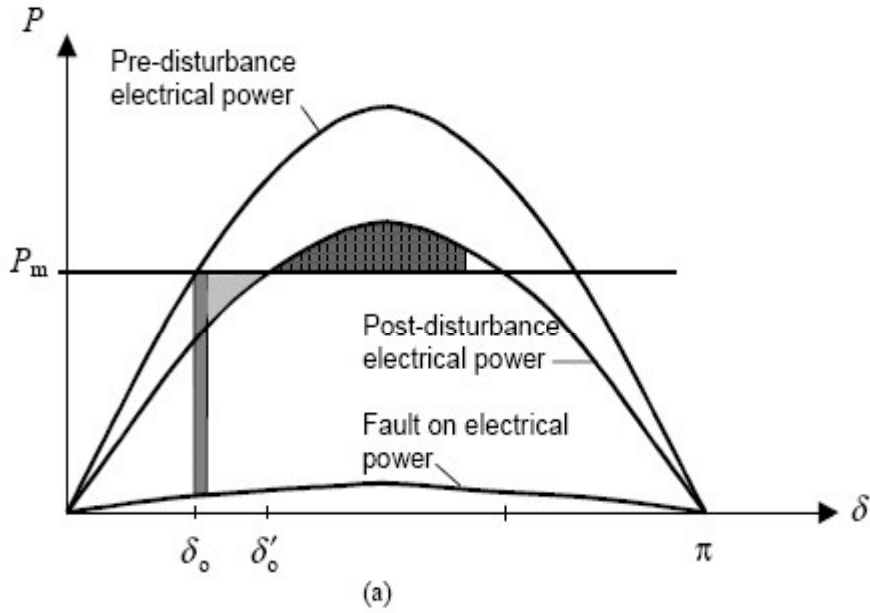


Figure 3-1 Angle stability illustration [26]

(a) Power angle curve and equal area criterion. Dark shading for acceleration energy during fault. Light shading for additional acceleration energy because of line outage. Black shading for deceleration energy. (b) Angle–speed phase plane. Dotted trajectory is for unstable case.

With the energy function analysis, it is possible to compute the swing energy associated with the system disturbances in simulation. Also, with the voltage phasor angle and frequency measurements from synchrophasors, it is possible to determine an estimate of the swing energy in real-time. Thus, the angle separation across the system can be quantified and control actions can be taken to stabilize the system. In [25], the critical energy of each generator in the system is predetermined by the off-line computations. In real-time simulation, the computation of the kinetic energy function of each generator is used to detect whether the generators are remain in boundary in order to analyze the system stability. The recent paper [28] proposed a synchronous phasor data

based energy function analysis in typical power transfer path with two generators. In our research, we carry out the potential energy function together with the kinetic energy function to define the total energy of each generator in the system. Computation of both energy functions in real-time is used to detect the system instability for the large power system with no restrictions on the size of the system or on the number of generators.

3.2. ALGORITHM

A partial energy function is one that computes the transient energy of a single generator (or subsystem) in a multi-machine power system. In partial energy function analysis, the transient energy for generator i , is defined as the integral of the power accelerating the generator's rotor,

$$PE_i = \int_{\theta_i} (PT_i - PG_i) d\theta_i \quad (3.1)$$

Transient energy can be resolved into Kinetic Energy, by

$$KE_i = H_i(\omega_i - 1)^2 \quad (3.2)$$

where ,

ω_i = rotor speed of generator

H_i = Inertia constant of generator

PT_i = torque

PG_i = MW generation of generator

θ_i = rotor angle

In our approach, we propose the real-time synchronous total energy of each generator in the system as the criterion to analyze the stability of the system. We define the total energy of each generator as TE_i ,

$$\text{where, } TE_i = KE_i + PE_i \quad (3.3)$$

Now, we simply use TE_i to analyze the stability of the system by observing whether TE_i values are remaining bounded. In practice, it is not convenient to get measurements of the rotor speed or angle. $\tilde{\omega}_i$ and $\tilde{\theta}_i$, representing the generator high side bus frequency and voltage angle, respectively, are introduced into the simulation. Also, we use the relative phase angle $\bar{\theta}_i$ which is the difference between the phase angle $\tilde{\theta}_i$ and the center angle θ_c introduced in Section 2.

3.3. ILLUSTRATION OF THE ALGORITHM IN THE TWO AREA SYSTEM

In the two area system, when we apply a three phase fault near Bus 8 and after some certain time we clear the fault and remove three of the four lines between Bus 7 and

Bus 8 at time 0.1 sec. This is a severe outage for the system and the details of the simulation results are shown below.

With the fault-on time 10 cycles, the potential energy, the kinetic energy, and the total energy of each generator are shown in Figure 3-2, Figure 3-3 and Figure 3-4, respectively.

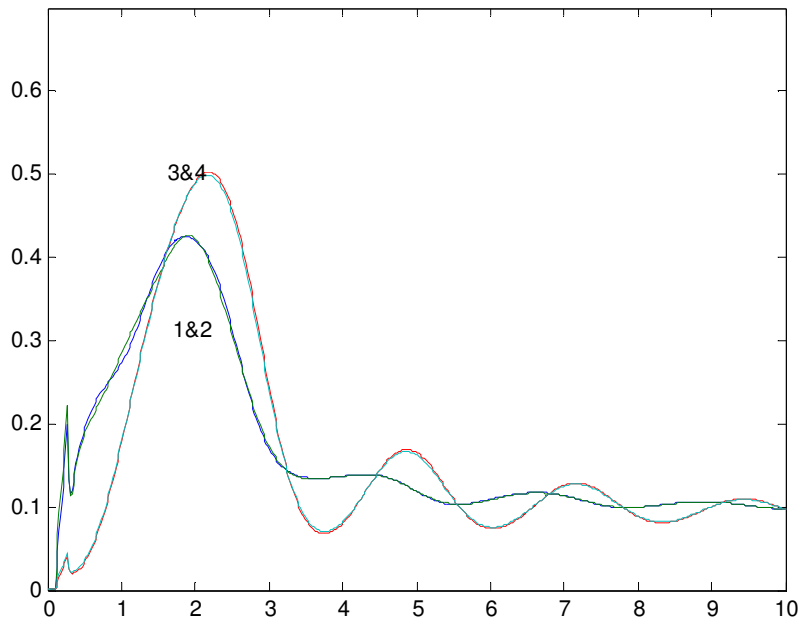


Figure 3-2 Kinetic energy of each generator (fault-on time=10 cycles)

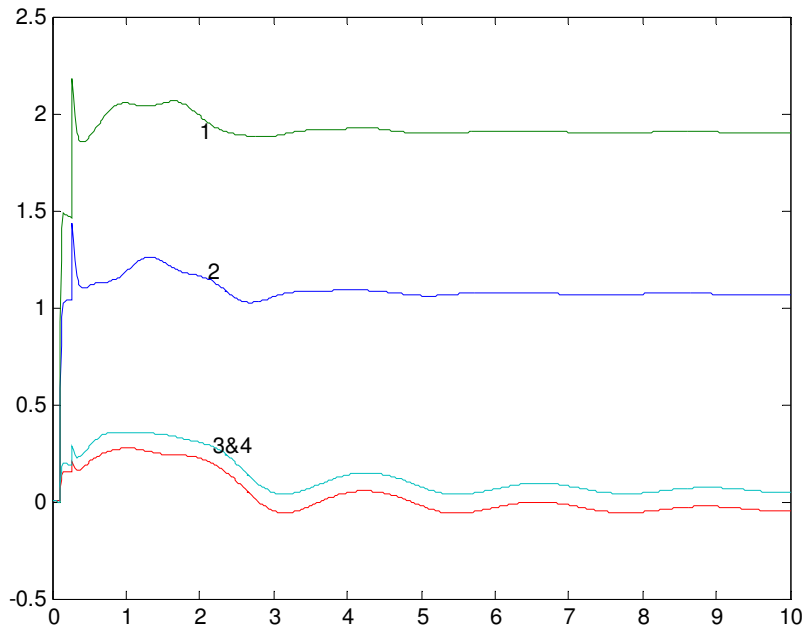


Figure 3-3 Potential energy of each generator (fault-on time=10 cycles)

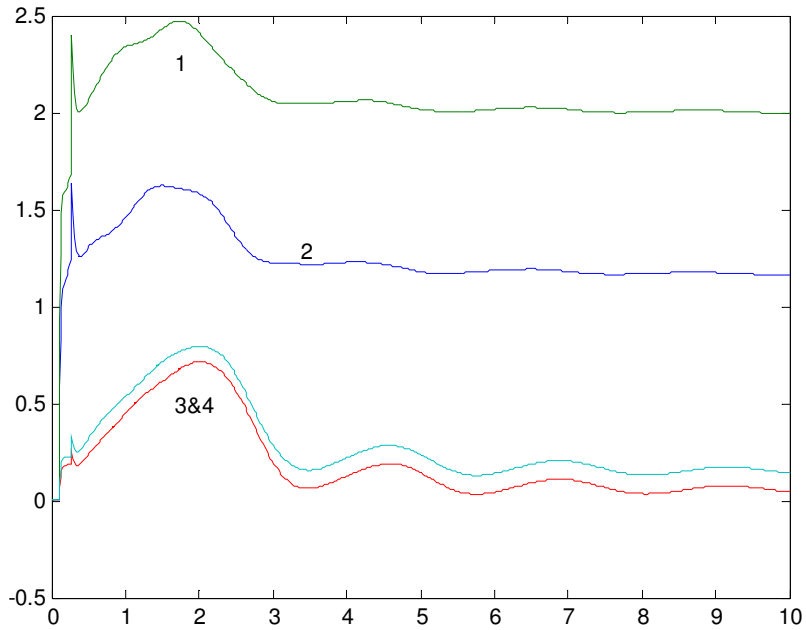


Figure 3-4 Total energy of each generator (fault-on time=10 cycles)

With the fault-on time 11 cycles, the potential energy, the kinetic energy, and the total energy of each generator are shown in Figure 3-5, Figure 3-6 and Figure 3-7,

respectively. If we put different thresholds for the four generators, we could implement some controls when the system goes unstable. For example, we set the thresholds as [2.0, 2.7, 1.0, 1.0], the time of each generator moving above thresholds is [1.68 sec, 1.52 sec, 9.68 sec, 9.56 sec], thus we can take some certain control to generator 1 to stabilize the system.

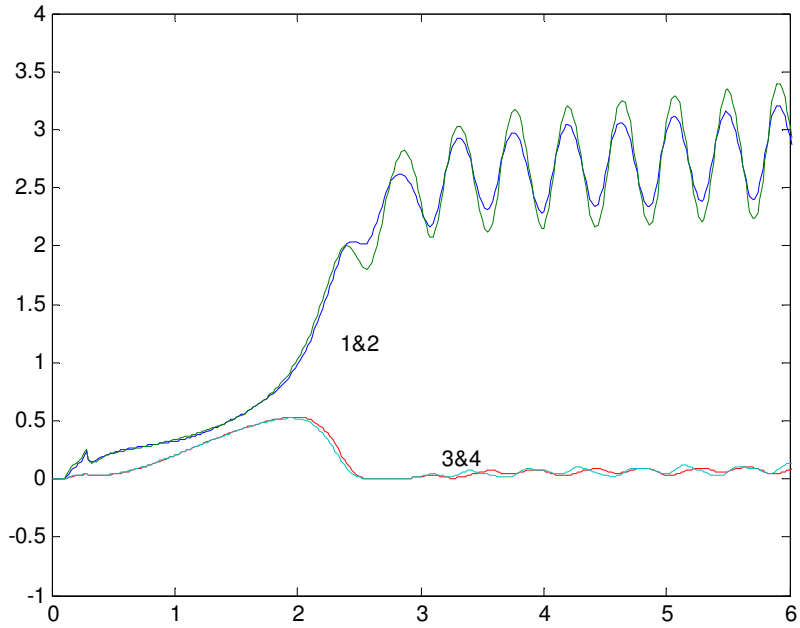


Figure 3-5 Kinetic energy of each generator (fault-on time=11 cycles)

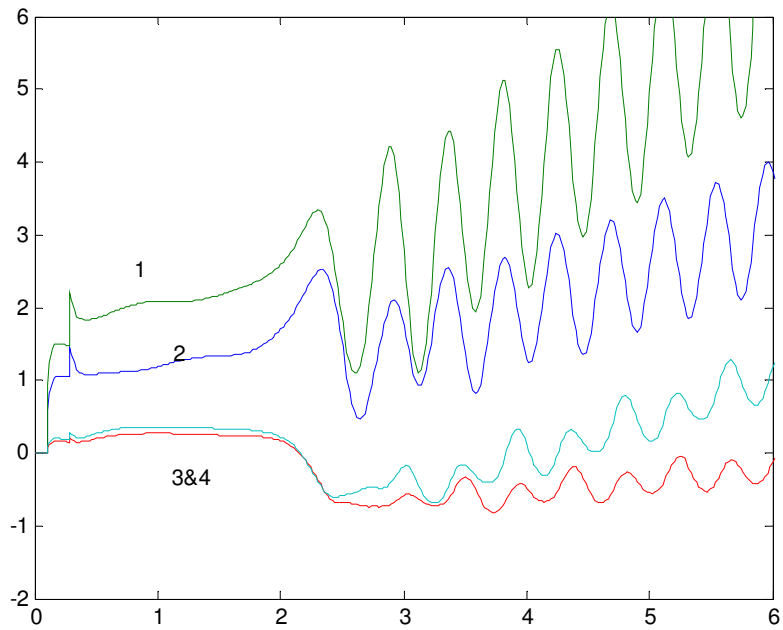


Figure 3-6 Potential energy of each generator (fault-on time=11 cycles)

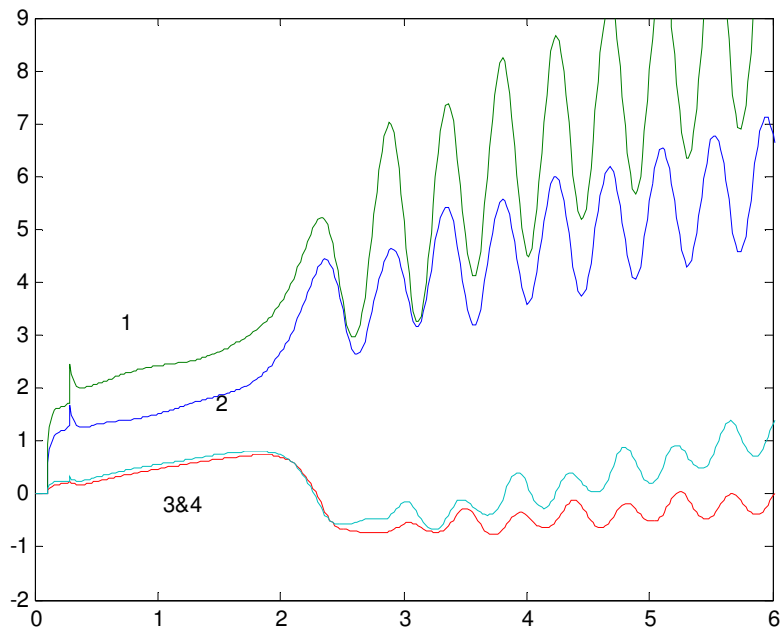


Figure 3-7 Total energy of each generator (fault-on time=11 cycles)

From the simulation results, it can be observed that the energy of each generator remains bounded in the stable cases and increases fast in the unstable cases. Thus, the

total energy function can be used as the criterion to analyze the stability of power system.

Now, we set the thresholds for the four generators as [2.0, 2.7, 1.0, 1.0], the simulation results with different fault-on times are shown in Table 3-1. Gen 2 is the first generator to move above the energy bound. Tripping Gen 2 (since it is accelerating as observed from the phase angle) and shedding 50% load of Area 2 (since it is decelerating as observed from the phase angle) at time 1.52 sec will stabilize the system. Table 3-2 lists the benefits that is provided by the algorithm in improving the system stability.

Table 3-1 Simulation results for the two area system

	10cycles	11cycles	12cycles	13cycles
Stability	Stable	Unstable	Unstable	Unstable
Critical Gen		2	2	2
T_control		1.52 sec	1.37 sec	1.21 sec

Table 3-2 Improvement on the system stability

Fault Bus	Line Removed	Fault Time(cycles) improvement
8	7-8	3
7	7-8	2

3.4. IMPLEMENTATION OF THE ALGORITHM IN THE 39 BUS SYSTEM

We also implement the algorithm in the 39 bus New England system. Now, we introduce an outage to explain the algorithm. There is a fault near Bus 4 on line 4-14, and the line 4-14 is removed as part of the fault clearing. With the fault-on time at 12 cycles, the potential energy, the kinetic energy, and the total energy of each generator are shown in Figure 3-8, Figure 3-9 and Figure 3-10, respectively. With the fault-on time at 13 cycles, the potential energy, the kinetic energy, and the total energy of each generator are shown in Figure 3-11, Figure 3-12 and Figure 3-13, respectively. Therefore, like for the two-area system, by assigning different thresholds to the generators, we could implement some remedial controls when the system goes unstable.

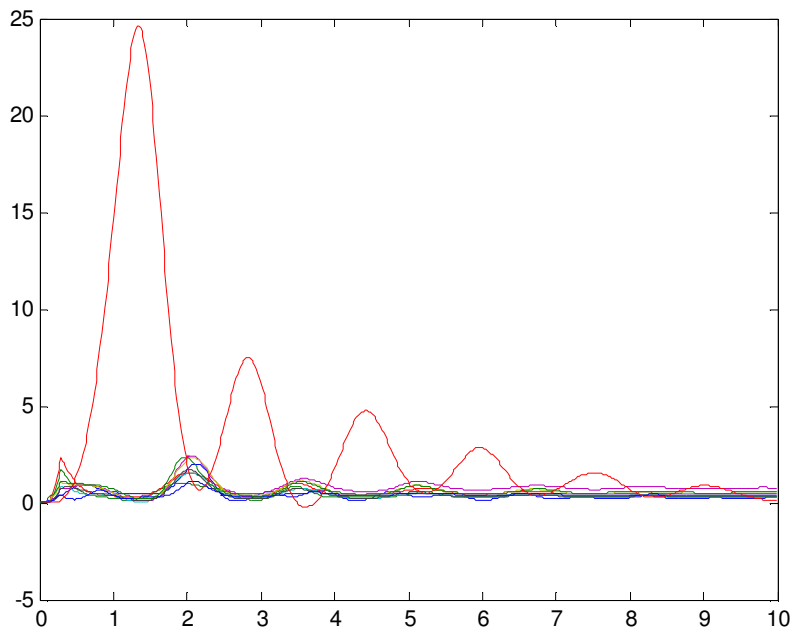


Figure 3-8 Potential energy of each generator (fault-on time=12 cycles)

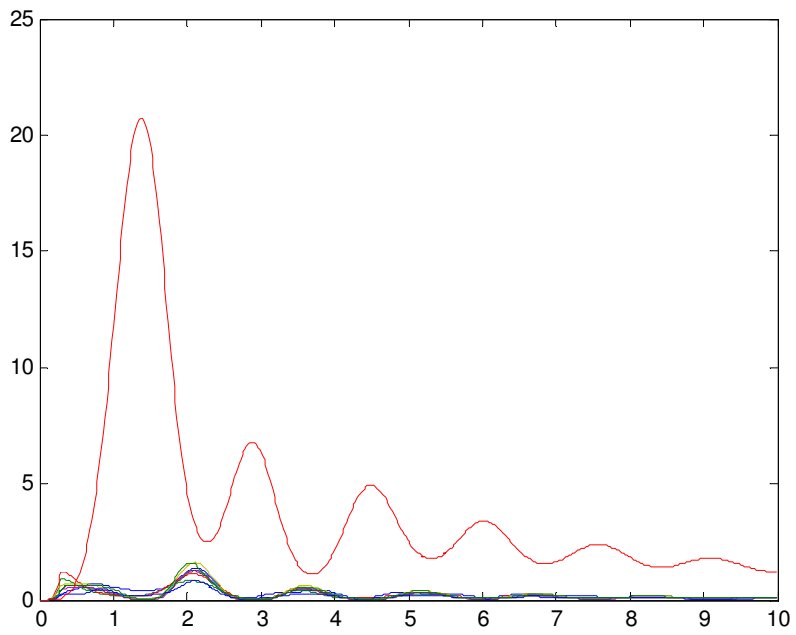


Figure 3-9 Kinetic energy of each generator (fault-on time=12 cycles)

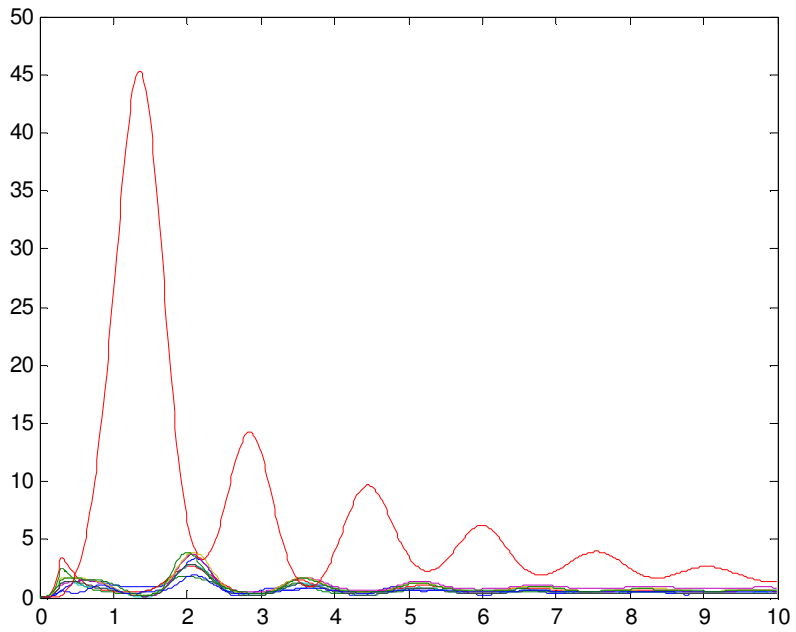


Figure 3-10 Total energy of each generator (fault-on time=12 cycles)

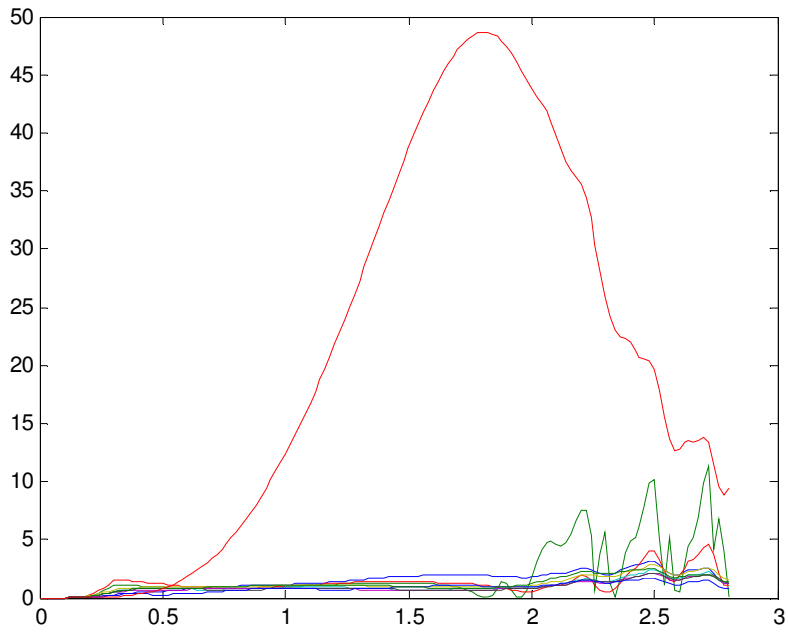


Figure 3-11 Potential energy of each generator (fault-on time=13 cycles)

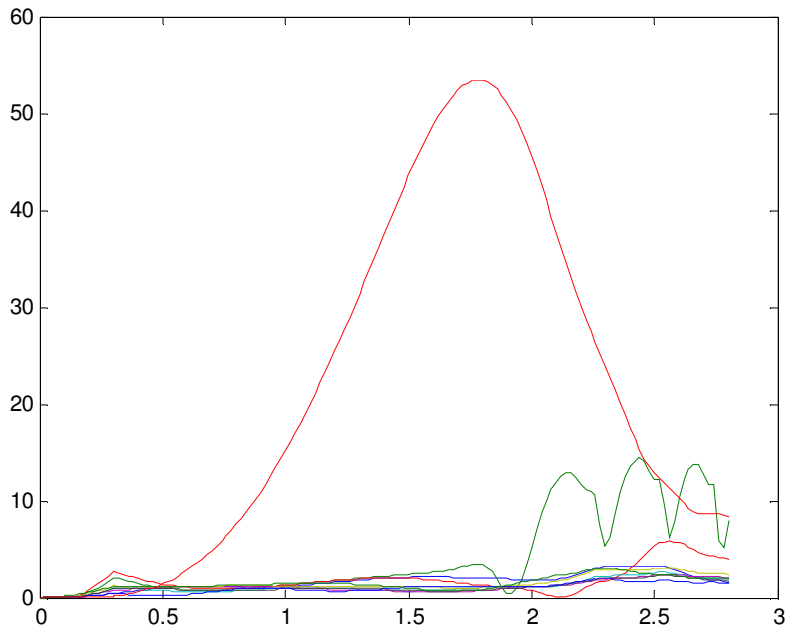


Figure 3-12 Kinetic energy of each generator (fault-on time=13 cycles)

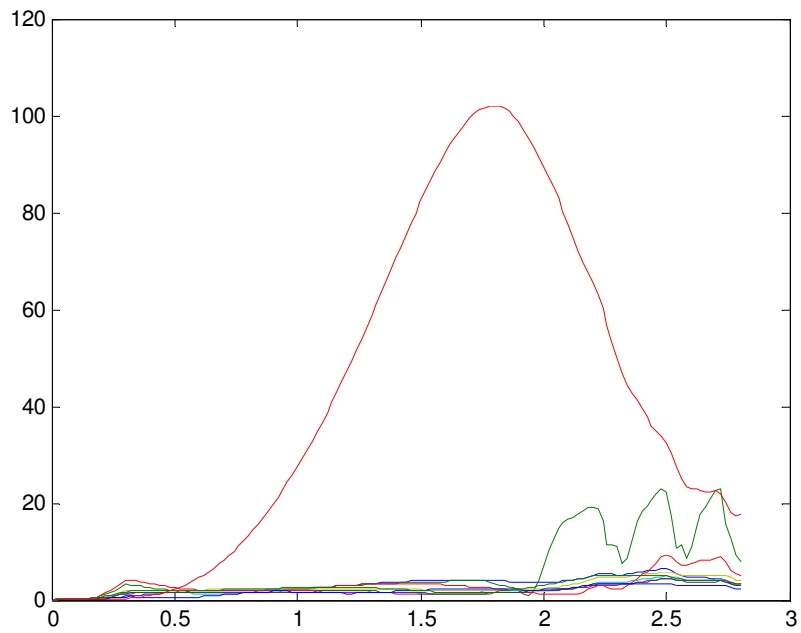


Figure 3-13 Total energy of each generator (fault-on time=13 cycles)

Since Gen 10 is much larger compared to the rest generators in capacities, the energy bound also needs to be set larger for Gen 10 compared to the rest. For example,

we set 50 as the threshold for Gen 10, and the energy threshold is 10 for the rest of the generators. The following table (Table 3-3) shows the simulation results. The fault time of each fault is the critical time when the system becomes unstable. The Gen is the critical generator that the algorithm singles out. Table 3-4 lists the benefits on the critical clearing times that the algorithm provides to the system stability. Considering the first contingency in Table 3-4, there is a three-phase fault near Bus 4 on line 4-14, and the line 4-14 is removed after clearing. The critical clearing time without the proposed control is 12 cycles. For this case, the energy function based algorithm identifies Gen 10 as the critical generator and a trip signal is issued by the control to Gen 10 at 1.09 seconds. Assuming that the generator then is tripped by the proposed controller, the system becomes transient stable for the clearing time of 13 cycles as well as 14 cycles. Compared to the 12 cycles for the original system with no control, the automatic controller as propose provides an improved critical clearing time by a margin of 2 cycles. Recalling the results from Table 2-3 and Table 2-4, we could find the energy function based algorithm consumes more time in identifying system instability as compared to the phase angle based algorithm of Section 2, so that the stability improvement for the energy function method is not as effective as for the phase angle based algorithm.

Table 3-3 Simulation results for the 39 bus system

Fault Bus	Line Removed	Fault Time(cycle s)	Gen tripped	Tripping time(sec)
4	4-14	13	10	1.09
14	4-14	13	10	1.13
4	4-5	12	10	1.31
3	3-4	12	10	0.99
4	3-4	11	10	1.03
5	5-6	11	2	1.23
6	5-6	10	2	1.37
2	2-25	7	9	1.41
25	2-25	6	9	1.32
16	16-19	5	4,5	0.58
19	19-16	5	4,5	0.52
21	16-21	9	10	1.02
16	16-21	7	10	0.92

Table 3-4 Improvement on the system stability

Fault Bus	Line Removed	Critical Clearing Time (cycles) improvement
4	4-14	2
14	4-14	2
4	4-5	3
3	3-4	1
4	3-4	1
5	5-6	1
6	5-6	1
2	2-25	0
25	2-25	0
16	16-19	0
19	19-16	0
21	16-21	1
16	16-21	1

3.5. CONCLUSIONS

The work reported in this section investigated the ability of energy function based on synchronized phase angle and bus frequency measurements to identify the emerging angle instabilities. The definition of the potential energy and the kinetic energy carry out new concepts of energy analysis for the real-time large power system control. The new algorithm is tested on both the two-area system and the 39 bus system.

4. SENSITIVITY STUDIES

In Sections 2 and 3, the two algorithms were proposed and tested in both the two area system and the 39 bus system. In this section, we discuss how sensitive the algorithms are on the simulation assumptions.

4.1. EFFECT OF DELAYS

In real-time control, we need to consider the typical delays involved in implementing the control. The delays include a) the transducer delay for the synchrophasor measurement, b) propagation delay from the PMU to the control center, c) delay at the data concentrator, d) processing delay, e) propagation delay from the control center to the circuit breaker, and f) circuit breaker delay. Suppose the average total delay which is the sum of the delays a) through e) above, is assumed to be 0.15 second or 150 milliseconds. Let us resimulate the example in Section 2 after including the delay of 150 milliseconds. Therefore, the new control time is simulated as 0.91 sec. The algorithm will still stabilize the system as shown in Figure 4-1. Essentially, the shorter time is consumed in communication, the more effective the algorithm will be as illustrated in Table 4-1.

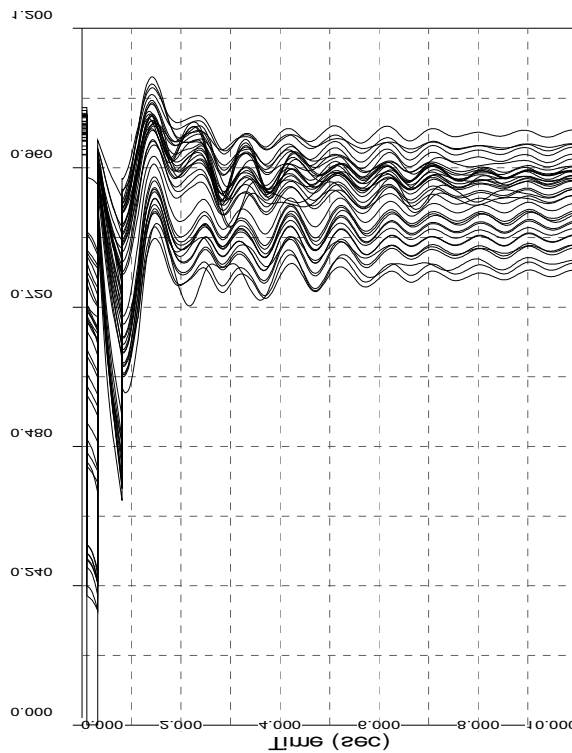


Figure 4-1 Bus voltages after tripping generator (communication time considered)

Table 4-1 Effects of communication time on system stability improvement

Communication time		0	0.10 sec	0.15 sec	0.20 sec
Improvement on the system stability (cycles)	Angle method	3	2	1	0
	Energy method	2	1	0	0

Based on the studies in Table 4-1, we recommend the use of dedicated communication network with minimal propagation delay over the use of open networks for the implementation of fast real-time algorithms such as the ones proposed in this paper.

4.2. LOSS OF MEASUREMENTS

Next, we take the 39 bus system example with 13 cycles clearing time in Section 2 and suppose the phase measurements of Bus 32 (not the critical one) are lost due to some unknown reasons. The simulation result will still give out Gen 10 as the critical generator and the control time is 0.80 sec. Table 4-2 illustrates the results with the loss of measurements. With ten measurements from the 39 bus system, loss of one or two angle measurements will not lead to a large detection error because of the method of weighted average used in the computation of COA.

Table 4-2 Simulation results in case of Loss of measurements

Loss of measurement	No loss	Bus32	Bus 30,32	Bus 30,32,35
Control time	0.76s	0.80 s	0.79 s	0.83 s
Critical Gen	Gen 10	Gen 10	Gen 10	Gen 10
Stability after control actions	Stable	Stable	Stable	Stable

4.3. CONCLUSIONS

The simulations in the section indicate the effectiveness of the algorithms even after the implementation delays are modeled, and in the face of loss of a few measurements. Further testing and analysis need to be carried out on both these questions in large power system models.

5. CONCLUSIONS

This paper presents algorithms for processing of phase angle measurements from across the system to decide whether any part or any control area within the system is speeding away from the rest. When the angle separations go above preset thresholds, remedial actions such as generation and load tripping are ordered by the stability controller to keep the areas in synchronism. This algorithm is meant to be a safety net when the normal RAS or SPS schemes have failed to operate for whatever reason and when the system is beginning to separate into islands. The proposed algorithm and the controller detect the fast separation of phase angles among the critical areas automatically using the synchrophasors and proceed to mitigate the instability by suitable switching actions. The paper tests the new algorithms with illustrative examples on standard IEEE test systems.

This paper also proposes the algorithm using real-time computation of energy functions to detect the system instability. When the system has large transient behaviors, the energy of the critical generators will move above their energy bound. This algorithm detects the critical generator's energy and leads to some witching controls. The energy function algorithm is also tested on standard IEEE test systems.

This paper introduces the algorithms, which can detect the system instability and also initiate suitable remedial control actions. However, the question on the amounts of the generation tripping and/or load shedding that is minimally required for stabilization, still needs to be further analyzed in future work. The computation and set-up of the thresholds for both algorithms also need to be tuned and the procedure streamlined in other larger test system models.

6. ACKNOWLEDGEMENTS

The research in this paper was supported by funding from Bonneville Power Administration (BPA), Power System Engineering Research Center (PSerc), and by Consortium for Electric Reliability Technology Solutions (CERTS). Partial funding from Pacificorp Inc. under the WSU Power Professorship program is also gratefully acknowledged.

REFERENCES

- [1] Dongchen Hu, "A wide-area control for mitigating angle instability in electric power systems", Masters thesis, School of EECS, Washington State University, Pullman, WA, December 2006.
- [2] "Final report on the August 14, 2003 blackout in the United States and Canada: Causes and recommendations," US–Canada Power System Outage Task Force, 2004.
- [3] V. Venkatasubramanian and Y. Li, "Analysis of the 1996 western american electric blackouts", *Proc. 2004 IREP Symposium Bulk Power Dynamics and Control -VI*, Cortina, Italy, August 2004.
- [4] P. Kundur, *Power System stability and control*, McGraw-Hill, 1994
- [5] C. W. Taylor, *Power system Voltage Stability*, McGraw-Hill, 1994
- [6] K. Tomsovic, D. Bakken, V. Venkatasubramanian, A. Bose, "Designing the Next Generation of Real-Time Control, Communication and Computations for Large Power Systems," *IEEE Proc. – Special Issue on Energy Infrastructure Systems, Proceedings of IEEE*, vol. 93, no. 5, May 2005.
- [7] C. Rehtanz, J. Bertsch, "Wide Area Measurement and Protection System for Emergency Voltage Stability Control," *Power Engineering Society Winter Meeting*, 2002. IEEE, vol. 2, pp. 842 – 847, Jan 2002.
- [8] I. Kamwa, R. Grondin, and Y. Hebert, "Wide-Area Measurement Based Stabilizing Control of Large Power Systems-A Decentralized/Hierarchical Approach," *IEEE Transactions on Power Systems*, Volume 16, Issue 1, pp. 136 – 153, Feb 2001.
- [9] C.W. Taylor, D.C.Erickson, K.E.Martin, R.E.Wilson, and V.Venkatasubramanian, "WACS-Wide-area stability and voltage control system: R&D and online demonstration", *Proceedings of the IEEE*, Vol.93, No.5, pp. 892-906, May 2005.
- [10] J. P. Paul, J. T. Leost, and J. M. Tesson, "Survey of the secondary voltage control in France: Present realization and investigations," *IEEE Trans. Power Systems*, vol. PWR-2, no. 2, pp. 505–511, May 1987.
- [11] S. Corsi, P. Marannino, N. Losignore, G. Moreschini, and G. Piccini, "Coordination between the reactive power scheduling function and the hierarchical voltage control of the EHV ENEL system," *IEEE Trans. Power Systems*, vol. 10, no. 2, pp. 686–694, May 1995.
- [12] H. Vu, P. Pruvot, C. Launay, and Y. Harmand, "An improved voltage control on large scale power system," *IEEE Trans. Power Systems*, vol. 11, no. 3, pp. 1295–1303, Aug. 1996.

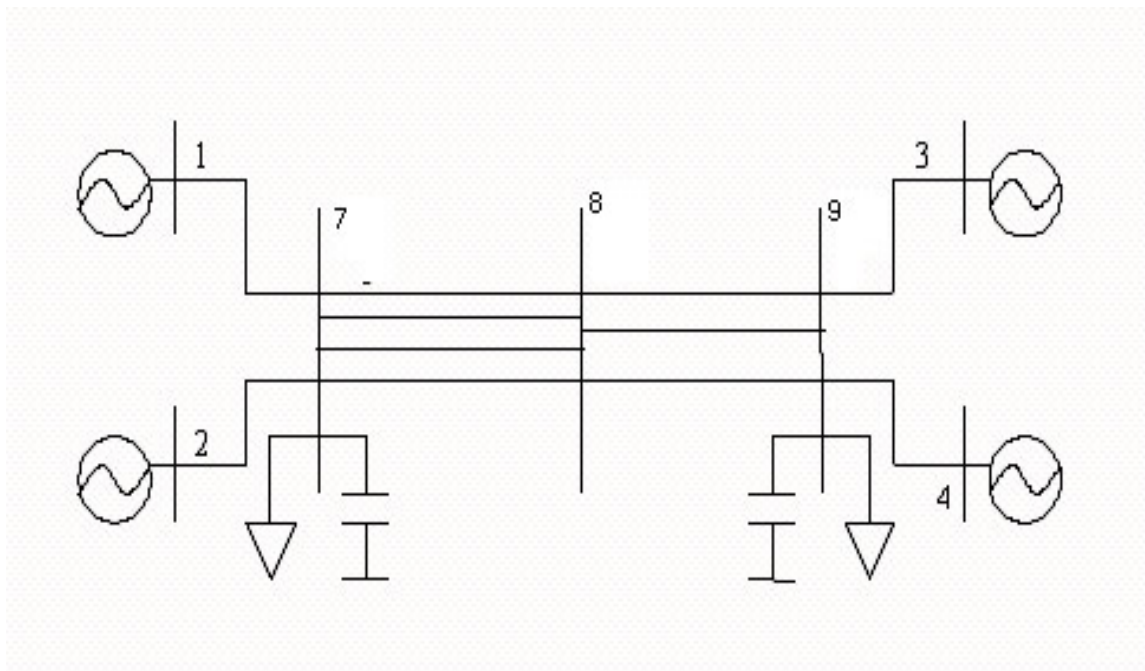
- [13] A. Zobian and M. Ilic, "A steady state voltage monitoring and control algorithm using localized least square minimization of load voltage deviations," *IEEE Trans. Power Systems*, vol. 11, no. 2, pp.929–938, May 1996.
- [14] C. Yu, Y. T. Yoon, M. Ilic, and A. Catelli, "On-line voltage regulation: The case of New England", *IEEE Trans. Power Systems*, vol. 14, no. 4, pp. 1477–1484, Nov. 1999.
- [15] Y. Chen, "Development of automatic slow voltage control for large power systems," *Ph.D. dissertation*, Washington State Univ., Pullman, 2001.
- [16] Zhang Yi, and K. Tomsovic, "Adaptive remedial action scheme based on transient energy analysis", *Power Systems Conference and Exposition 2004*, IEEE PES 10-13, pp. 925 - 931 vol.2, Oct. 2004.
- [17] CIGRE TF 38-02-17, Advanced Angle Stability Controls, *GIGRE Brochure No.155*, April 2000.
- [18] P.D. Aylett. "The Energy Integral Criterion of Transient Stability Limits of Power Systems." *Proceedings IEEE*, 105(C), pp. 527-536, 1958,
- [19] E.W. Kimbark. "Power System Stability", John Wiley & Sons, Inc., New York, NY. 1945.
- [20] T. Athay, V.R. Sherket, R. Podmore, S. Virmani, and C. Puech. "A Practical Method for Direct Analysis of Transient Stability." *IEEE Trans. PAS-98*, pp. 573-584, 1979,
- [21] A. A. Fouad and S. E. Stanton, "Transient Stability of a Multi- machine Power System, Part I: Investigation of System Trajectories," *IEEE Transactions PAS-100*, pp. 3408-3416, 1981.
- [22] A. A. Fouad and S. E. Stanton, "Transient Stability of a Multi- machine Power System, Part 11: Critical Transient Energy," *IEEE Transactions PAS-100*, pp. 3417-3424, 1981.
- [23] Michel, A. Fouad, A. Vittal, V., "Power system transient stability using individual machine energy functions", *IEEE Transactions on Circuits and Systems*, Volume 30, Issue 5, pp. 266 – 276, May 1983.
- [24] S. E. Stanton, "Transient Stability Monitoring for Electric Power Systems Using Partial Energy Functions," *IEEE Transactions on Power Systems*, Vol. 4, No. 4, pp. 1389-1395, 1989.
- [25] S. E. Stanton and W. P. Dykas, "Analysis of a Local Transient Control Action by Partial Energy Functions," *IEEE Transactions on Power Systems*, Vol. 4, No. 3, pp. 996-1002, 1989.

[26] A. A. Fouad and V. Vittal. "Power system Transient Stability Analysis Using the Transient Energy Function Method", Prentice Hall, Inc., 1992.

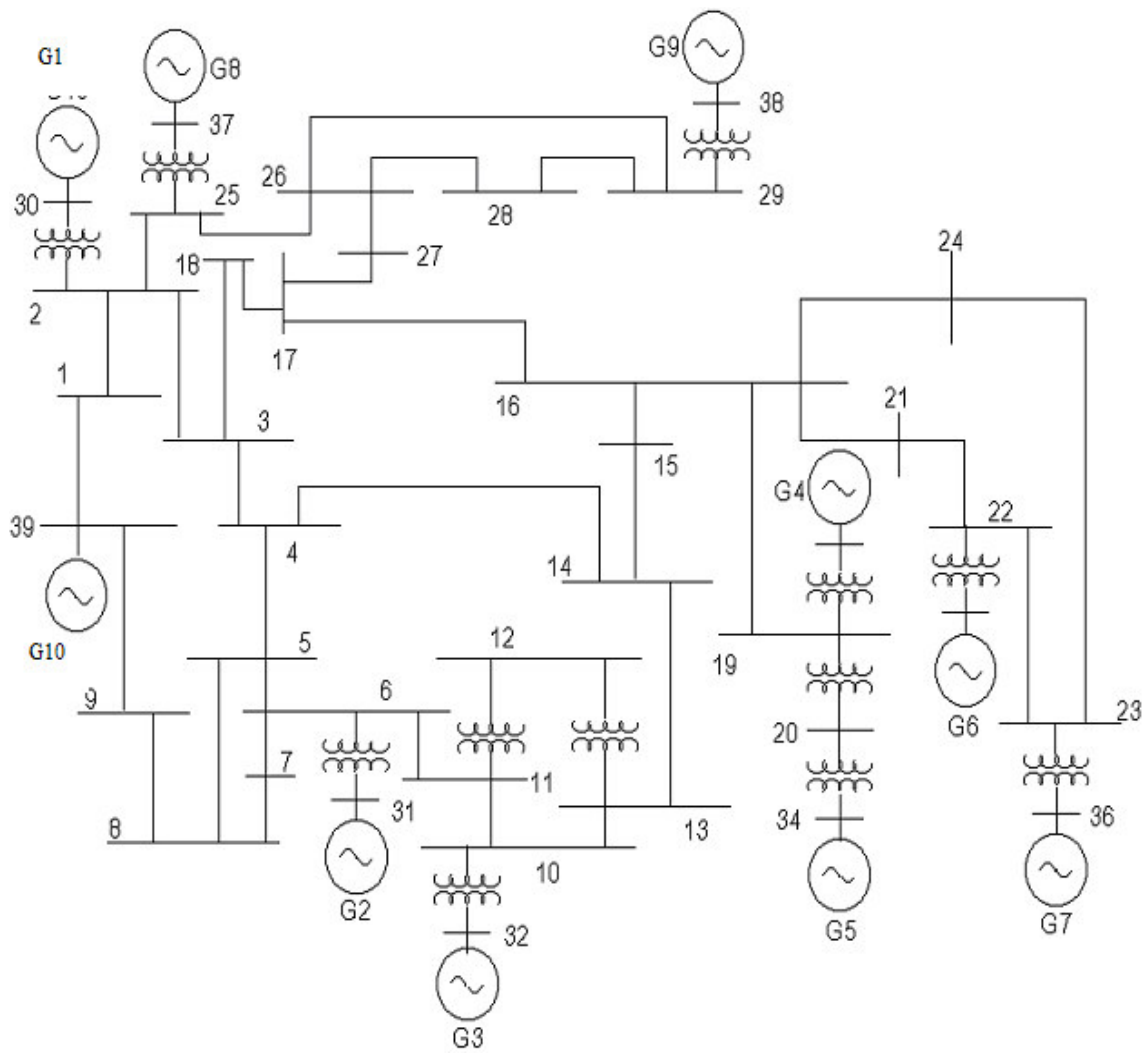
[27] S.E. Stanton, C. Slivinsky, K. Martin, and J. Nordstrom, "Application of phasor measurements and partial energy analysis in stabilizing large disturbances", *IEEE Transactions on Power Systems*, Volume 10, Issue 1, pp. 297 – 306, Feb 1995.

[28] J.H. Chow, A. Chakraborty, M. Arcak, B. Bhargava, and A. Salazar, "Synchronized Phasor Data Based Energy Function Analysis of Dominant Power Transfer Paths in Large Power Systems", *IEEE Summer Power Meeting*, Montreal, Canada, June 2006.

APPENDICES



Appendix A. One line diagram of the two-area test system [4]



Appendix B. One line diagram of the 39 bus New England test system